Inhibitory effect of eslicarbazepine acetate and S-licarbazepine on $Na_v1.5$ channels

Theresa K. Leslie[1], Lotte Brückner [1], Sangeeta Chawla[1,2], William J. Brackenbury[1,2*]

[1]Department of Biology, University of York, Heslington, York, YO10 5DD, UK

[2]York Biomedical Research Institute, University of York, Heslington, York, YO10 5DD, UK

*** Correspondence:** Dr William J. Brackenbury, Department of Biology and York Biomedical Research Institute, University of York, Wentworth Way, Heslington, York YO10 5DD, UK. Email: william.brackenbury@york.ac.uk. Tel: +44 1904 328284.

Keywords: Anticonvulsant, cancer, epilepsy, eslicarbazepine acetate, $Na_v1.5$, S-licarbazepine, voltage-gated Na^+ channel.

Abstract

Eslicarbazepine acetate (ESL) is a dibenzazepine anticonvulsant approved as adjunctive treatment for partial-onset epileptic seizures. Following first pass hydrolysis of ESL, S-licarbazepine (S-Lic) represents around 95 % of circulating active metabolites. S-Lic is the main enantiomer responsible for anticonvulsant activity and this is proposed to be through the blockade of voltage-gated Na^+ channels (VGSCs). ESL and S-Lic both have a voltage-dependent inhibitory effect on the Na^+ current in N1E-115 neuroblastoma cells expressing neuronal VGSC subtypes including $Na_v1.1$, $Na_v1.2$, $Na_v1.3$, $Na_v1.6$ and $Na_v1.7$. ESL has not been associated with cardiotoxicity in healthy volunteers, although a prolongation of the electrocardiographic PR interval has been observed, suggesting that ESL may also inhibit cardiac $Na_v1.5$ isoform. However, this has not previously been studied. Here, we investigated the electrophysiological effects of ESL and S-Lic on $Na_v1.5$ using whole-cell patch clamp recording. We interrogated two model systems: (1) MDA-MB-231 metastatic breast carcinoma cells, which endogenously express the 'neonatal' $Na_v1.5$ splice variant, and (2) HEK-293 cells stably over-expressing the 'adult' $Na_v1.5$ splice variant. We show that both ESL and S-Lic inhibit transient and persistent Na^+ current, hyperpolarise the voltage-dependence of fast inactivation, and slow the recovery from channel inactivation. These findings highlight, for the first time, the potent inhibitory effects of ESL and S-Lic on the $Na_v1.5$ isoform, suggesting a possible explanation for the prolonged PR interval observed in patients on ESL treatment. Given that numerous cancer cells have also been shown to express $Na_v1.5$, and that VGSCs potentiate invasion and metastasis, this study also paves the way for future investigations into ESL and S-Lic as potential invasion inhibitors.

1 Introduction

Eslicarbazepine acetate (ESL) is a member of the dibenzazepine anticonvulsant family of compounds which also includes oxcarbazepine and carbamazepine (1). ESL has been approved by the European Medicines Agency and the United States Federal Drug Administration as an adjunctive treatment for partial-onset epileptic seizures (2). ESL is administered orally and rapidly undergoes first pass hydrolysis to two stereoisomeric metabolites, R-licarbazepine and S-licarbazeine (S-Lic; also known as eslicarbazepine; Figure 1A, B) (3-5). S-Lic represents around 95 % of circulating active metabolites following first pass hydrolysis of ESL and is the enantiomer responsible for

anticonvulsant activity (6, 7). S-Lic also has improved blood brain barrier penetration compared to R-licarbazepine (8). Although S-Lic has been shown to inhibit T type Ca^{2+} channels (9), its main activity is likely through blockade of voltage-gated Na^+ channels (VGSCs) (10). ESL offers several clinical advantages over other older VGSC-inhibiting antiepileptic drugs, e.g. carbamazepine, phenytoin; it has a favourable safety profile (10, 11), reduced induction of hepatic cytochrome P450 enzymes (12), low potential for drug-drug interactions (13, 14), and takes less time to reach a steady state plasma concentration (15).

VGSCs are composed of a pore-forming α subunit in association with one or more auxiliary β subunits, the latter modulating channel gating and kinetics in addition to functioning as cell adhesion molecules (16). There are nine α subunits ($Na_v1.1$-$Na_v1.9$), and four β subunits (β1-4) (17, 18). In postnatal and adult CNS neurons, the predominant α subunits are the tetrodotoxin-sensitive $Na_v1.1$, $Na_v1.2$ and $Na_v1.6$ isoforms (19) and it is therefore on these that the VGSC-inhibiting activity of ESL and S-Lic has been described. In the murine neuroblastoma N1E-115 cell line, which expresses $Na_v1.1$, $Na_v1.2$, $Na_v1.3$, $Na_v1.6$ and $Na_v1.7$, ESL and S-Lic both have a voltage-dependent inhibitory effect on the Na^+ current (10, 20). In this cell model, S-Lic has no effect on the voltage-dependence of fast inactivation, but significantly hyperpolarises the voltage-dependence of slow inactivation (10). S-Lic also has a lower affinity for VGSCs in the resting state than carbamazepine or oxcarbazepine, thus potentially improving its therapeutic window over first- and second-generation dibenzazepine compounds (10). In acutely isolated murine hippocampal CA1 neurons, which express $Na_v1.1$, $Na_v1.2$ and $Na_v1.6$ (21-23), S-Lic significantly reduces the persistent Na^+ current, a very slow-inactivating component ~1 % the size of the peak transient Na^+ current (24, 25). Moreover, in contrast to carbamazepine, this effect is maintained in the absence of β1 (24, 26).

In healthy volunteers, ESL has not been associated with cardiotoxicity and the QT interval remains unchanged on treatment (27). However, a prolongation of the PR interval has been observed (27), suggesting that caution should be exercised in patients with cardiac conduction abnormalities (13). Prolongation of the PR interval suggests that ESL may also inhibit the cardiac $Na_v1.5$ isoform, although this has not previously been studied. $Na_v1.5$ is not only responsible for the initial depolarisation of the cardiac action potential (28), but is also expressed in breast and colon carcinoma cells, where the persistent Na^+ current promotes invasion and metastasis (29-32). Inhibition of $Na_v1.5$ with phenytoin or ranolazine decreases tumour growth, invasion and metastasis (33-35). Thus, it is of interest to specifically understand the effect of ESL on the $Na_v1.5$ isoform.

In the present study we investigated the electrophysiological effects of ESL and S-Lic on $Na_v1.5$ [1] endogenously expressed in the MDA-MB-231 metastatic breast carcinoma cell line, and [2] stably over-expressed in HEK-293 cells. We show that both ESL and S-Lic inhibit transient and persistent Na^+ current, hyperpolarise the voltage-dependence of fast inactivation, and slow the recovery from channel inactivation. These findings highlight, for the first time, the potent inhibitory effects of ESL and S-Lic on the $Na_v1.5$ isoform.

2 Materials and methods

2.1 Pharmacology

ESL (Tokyo Chemical Industry UK Ltd) was dissolved in DMSO to make a stock concentration of 67 mM. S-Lic (Tocris) was dissolved in DMSO to make a stock concentration of 300 mM. Both drugs were diluted to a working concentration of 300 μM in extracellular recording solution. The concentration of DMSO in the recording solution was 0.45 % for ESL and 0.1 % for S-Lic. Equal

concentrations of DMSO were used in the control solutions. DMSO (0.45 %) had no effect on the Na^+ current (Supplementary Figure 1).

2.2 Cell culture

MDA-MB-231 cells and HEK-293 cells stably expressing $Na_v1.5$ (a gift from L. Isom, University of Michigan) were grown in Dulbecco's modified eagle medium supplemented with 5 % FBS and 4 mM L-glutamine (36). Molecular identity of the MDA-MB-231 cells was confirmed by short tandem repeat analysis (37). Cells were confirmed as mycoplasma-free using the DAPI method (38). Cells were seeded onto glass coverslips 48 h before electrophysiological recording.

2.3 Electrophysiology

Plasma membrane Na^+ currents were recorded using the whole-cell patch clamp technique, using methods described previously (32, 35). Patch pipettes made of borosilicate glass were pulled using a P-97 pipette puller (Sutter Instrument) and fire-polished to a resistance of 3-5 MΩ when filled with intracellular recording solution. The extracellular recording solution for MDA-MB-231 cells contained (in mM): 144 NaCl, 5.4 KCl, 1 $MgCl_2$, 2.5 $CaCl_2$, 5.6 D-glucose and 5 HEPES (adjusted to pH 7.2 with NaOH). For the extracellular recording solution for HEK-293 cells expressing $Na_v1.5$, the extracellular [Na^+] was reduced to account for the much larger Na^+ currents and contained (in mM): 60 NaCl, 84 Choline Cl, 5.4 KCl, 1 $MgCl_2$, 2.5 $CaCl_2$, 5.6 D-glucose and 5 HEPES (adjusted to pH 7.2 with NaOH). The intracellular recording solution contained (in mM): 5 NaCl, 145 CsCl, 2 $MgCl_2$, 1 $CaCl_2$, 10 HEPES, 11 EGTA, (adjusted to pH 7.4 with CsOH) (39). Voltage clamp recordings were made at room temperature using a Multiclamp 700B amplifier (Molecular Devices) compensating for series resistance by 40–60%. Currents were digitized using a Digidata 1440A interface (Molecular Devices), low pass filtered at 10 kHz, sampled at 50 kHz and analysed using pCLAMP 10.7 software (Molecular Devices). Leak current was subtracted using a P/6 protocol (40). Extracellular recording solution ± drugs was applied to the recording bath at a rate of ~1.5 ml/min using a ValveLink 4-channel gravity perfusion controller (AutoMate Scientific). Each new solution was allowed to equilibrate in the bath for ~4 min following switching prior to recording at steady state.

2.4 Voltage clamp protocols

Cells were clamped at a holding potential of -120 mV or -80 mV for ≥ 250 ms, dependent on experiment (detailed in the Figure legends). Five main voltage clamp protocols were used, as follows:

1. To assess the effect of drug perfusion and wash-out on peak current in real time, a simple one-step protocol was used where cells were held at -120 mV or -80 mV for 250 ms and then depolarised to -10 mV for 50 ms.

2. To assess the voltage-dependence of activation, cells were held at -120 mV for 250 ms and then depolarised to test potentials in 10 mV steps between -120 mV and +30 mV for 50 ms. The voltage of activation was taken as the most negative voltage which induced a visible transient inward current.

3. To assess the voltage-dependence of steady-state inactivation, cells were held at -120 mV for 250 ms followed by prepulses for 250 ms in 10 mV steps between -120 mV and +30 mV and a test pulse to -10 mV for 50 ms.

4. To assess use-dependent block, cells were held at -120 mV for 250 ms and then depolarised to 0 mV at a frequency of 50 Hz, with each depolarisation pulse lasting 5 ms.

5. To assess recovery from fast inactivation, cells were held at -120 mV for 250 ms, and then depolarised twice to 0 mV for 25 ms, returning to -120 mV for the following intervals between depolarisations (in ms): 1, 2, 3, 5, 7, 10, 15, 20, 30, 40, 50, 70, 100, 150, 200, 250, 350, 500. In each case, the second current was normalised to the initial current and plotted against the interval time.

2.5 Curve fitting and data analysis

To study the voltage-dependence of activation, current-voltage (I-V) relationships were converted to conductance using the following equation:

$G = I / (V_m - V_{rev})$, where G is conductance, I is current, V_m is the membrane voltage and V_{rev} is the reversal potential for Na^+ derived from the Nernst equation. Given the different recording solutions used, V_{rev} for Na^+ was +85 mV for MDA-MB-231 cells and +63 mV for HEK-$Na_v1.5$ cells.

The voltage-dependence of conductance and availability were normalised and fitted to a Boltzmann equation:

$G = G_{max} / (1 + \exp((V_{1/2} - V_m) / k))$, where G_{max} is the maximum conductance, $V_{1/2}$ is the voltage at which the channels are half activated/inactivated, V_m is the membrane voltage and k is the slope factor.

Recovery from inactivation data ($I_t / I_{t=0}$) were normalised, plotted against recovery time (Δt) and fitted to a single exponential function:

$\tau = A_1 + A_2 \exp(-t / t_0)$, where A_1 and A_2 are the coefficients of decay of the time constant (τ), t is time and t_0 is a time constant describing the time dependence of τ.

The time course of inactivation was fitted to a double exponential function:

$I = A_f \exp(-t / \tau_f) + A_s \exp(-t / \tau_s) + C$, where A_f and A_s are maximal amplitudes of the slow and fast components of the current, τ_f and τ_s are the fast and slow decay time constants and C is the asymptote.

2.6 Statistical analysis

Data are presented as mean and SEM unless stated otherwise. Statistical analysis was performed on the raw data using GraphPad Prism 8.4.0. Pairwise statistical significance was determined with Student's paired *t*-tests. Multiple comparisons were made using ANOVA and Tukey post-hoc tests, unless stated otherwise. Results were considered significant at $P < 0.05$.

3 Results

3.1 Effect of eslicarbazepine acetate and S-licarbazepine on transient and persistent Na^+ current

Several studies have clearly established the inhibition of neuronal VGSCs ($Na_v1.1$, $Na_v1.2$, $Na_v1.3$, $Na_v1.6$, $Na_v1.7$ and $Na_v1.8$) by ESL and its active metabolite S-Lic (10, 20, 24, 41). Given that ESL

prolongs the PR interval (27), potentially via inhibiting the cardiac $Na_v1.5$ isoform, together with the interest in inhibiting $Na_v1.5$ in carcinoma cells to reduce invasion and metastasis (33, 34, 42-44), it is also relevant to evaluate the electrophysiological effects of ESL and S-Lic on this isoform. We therefore evaluated the effect of both compounds on $Na_v1.5$ current properties using whole-cell patch clamp recording, employing a two-pronged approach: (1) recording $Na_v1.5$ currents endogenously expressed in the MDA-MB-231 breast cancer cell line (29, 30, 45), and (2) recording from $Na_v1.5$ stably over-expressed in HEK-293 cells (HEK-$Na_v1.5$) (46).

Initially, we evaluated the effect of both compounds on the size of the peak Na^+ current in MDA-MB-231 cells. Na^+ currents were elicited by depolarising the membrane potential (V_m) to -10 mV from a holding potential (V_h) of -120 mV or -80 mV. Application of the prodrug ESL (300 µM) reversibly inhibited the transient Na^+ current by 49.6 ± 3.2 % when the V_h was -120 mV ($P < 0.001$; n = 13; ANOVA + Tukey test; Figure 2A, D). When V_h was set to -80 mV, ESL reversibly inhibited the transient Na^+ current by 79.5 ± 4.5 % ($P < 0.001$; n = 12; ANOVA + Tukey test; Figure 2C, E). We next assessed the effect of ESL in HEK-$Na_v1.5$ cells. Application of ESL inhibited $Na_v1.5$ current by 74.7 ± 4.3 % when V_h was -120 mV ($P < 0.001$; n = 12; Figure 2F, I) and by 90.5 ± 2.8 % when V_h was -80 mV ($P < 0.001$; n = 14; Figure 2H, J). However, the inhibition was only partially reversible ($P < 0.001$; n = 14; Figure 2F, H-J). Together, these data suggest that ESL preferentially inhibited $Na_v1.5$ in the open or inactivated state, since the current inhibition was greater at more depolarised V_h.

We next tested the effect of the active metabolite S-Lic. S-Lic (300 µM) inhibited the transient Na^+ current in MDA-MB-231 cells by 44.4 ± 6.1 % when the V_h was -120 mV ($P < 0.001$; n = 9; ANOVA + Tukey test; Figure 3A, D). When V_h was set to -80 mV, S-Lic (300 µM) inhibited the transient Na^+ current by 73.6 ± 4.1 % ($P < 0.001$; n = 10; ANOVA + Tukey test; Figure 3C, E). However, the inhibition caused by S-Lic was only partially reversible ($P < 0.05$; n = 10; ANOVA + Tukey test; Figure 3A, C-E). In HEK-$Na_v1.5$ cells, S-Lic inhibited $Na_v1.5$ current by 46.4 ± 3.9 % when V_h was -120 mV ($P < 0.001$; n = 13; ANOVA + Tukey test; Figure 3F, I) and by 74.0 ± 4.2 % when V_h was -80 mV ($P < 0.001$; n = 12; ANOVA + Tukey test; Figure 3H, J). Furthermore, the inhibition in HEK-$Na_v1.5$ cells was not reversible over the duration of the experiment. Together, these data show that channel inhibition by S-Lic was also more effective at more depolarised V_h. However, unlike ESL, channel blockade by S-Lic persisted after washout, suggesting higher target binding affinity for the active metabolite.

We also assessed the effect of both compounds on the persistent Na^+ current measured 20-25 ms after depolarisation to -10 mV from -120 mV. In MDA-MB-231 cells, ESL inhibited the persistent Na^+ current by 77 ± 34 % although the reduction was not statistically significant ($P = 0.13$; n = 12; paired t test; Figure 2B, Table 1). In HEK-$Na_v1.5$ cells, ESL inhibited persistent current by 76 ± 10 % ($P < 0.01$; n = 12; paired t test; Figure 2G, Table 1). S-Lic inhibited the persistent Na^+ current in MDA-MB-231 cells by 66 ± 16 % ($P < 0.05$; n = 9; paired t test; Figure 3B, Table 2). In HEK-$Na_v1.5$ cells, S-Lic inhibited persistent current by 35 ± 16 % ($P < 0.05$; n = 11; Figure 3G, Table 2). In summary, both ESL and S-Lic also inhibited the persistent Na^+ current.

3.2 Effect of eslicarbazepine acetate and S-licarbazepine on voltage dependence of activation and inactivation

We next investigated the effect of ESL (300 µM) and S-Lic (300 µM) on the I-V relationship in MDA-MB-231 and HEK-$Na_v1.5$ cells. A V_h of -120 mV was used for subsequent analyses to ensure that the elicited currents were sufficiently large for analysis of kinetics and voltage dependence,

204 particularly for MDA-MB-231 cells, which display smaller peak Na^+ currents (Tables 1, 2). Neither
205 ESL nor S-Lic had any effect on the threshold voltage for activation (Figure 4A-D; Tables 1, 2). ESL
206 also had no effect on the voltage at current peak in either cell line (Figure 4A-D; Tables 1, 2).
207 Although S-Lic had no effect on voltage at current peak in MDA-MB-231 cells, it significantly
208 hyperpolarised in HEK-$Na_v1.5$ cells from -18.0 ± 4.2 mV to -30.0 ± 5.6 mV ($P < 0.001$; n = 9; paired
209 t test; Figure 4A-D; Tables 1, 2).

210 ESL had no significant effect on the half-activation voltage (V½) or slope factor (k) for activation in
211 MDA-MB-231 cells (Figure 5A; Table 1). The activation k in HEK-$Na_v1.5$ cells was also unchanged
212 but the activation V½ was significantly hyperpolarised by ESL from -39.4 ± 1.3 to -44.2 ± 1.8 mV (P
213 < 0.05; n = 10; paired t test; Figure 5B; Table 1). S-Lic also had no significant effect on the activation
214 V½ or k in MDA-MB-231 cells (Figure 5C; Table 2). However, the V½ of activation in HEK-$Na_v1.5$
215 cells was significantly hyperpolarised from -32.8 ± 3.1 mV to -40.5 ± 3.4 mV ($P < 0.01$; n = 9; paired
216 t test; Figure 5D; Table 2) and k changed from 5.9 ± 0.9 mV to 4.5 ± 1.1 mV ($P < 0.05$; n = 9; paired
217 t test; Figure 5D; Table 2).

218 As regards steady-state inactivation, in MDA-MB-231 cells, ESL significantly hyperpolarised the
219 inactivation V½ from -80.6 ± 0.7 mV to -86.7 ± 1.2 mV ($P < 0.001$; n = 13; paired t test) without
220 affecting inactivation k (Figure 5A; Table 1). ESL also hyperpolarised the inactivation V½ in HEK-
221 $Na_v1.5$ cells from -78.2 ± 2.5 mV to -88.3 ± 2.7 mV ($P < 0.001$; n = 10; paired t test), and changed
222 the inactivation k from -6.9 ± 0.4 mV to -9.8 ± 0.7 mV ($P < 0.001$; n = 10; paired t test; Figure 5B;
223 Table 1). S-Lic also significantly hyperpolarised the inactivation V½ in MDA-MB-231 cells from -
224 71.8 ± 2.5 mV to -76.8 ± 2.2 mV ($P < 0.05$; n = 7; paired t test) without affecting inactivation k
225 (Figure 5C; Table 2). However, the inactivation V½ in HEK-$Na_v1.5$ cells was not significantly
226 altered by S-Lic, although the inactivation k significantly changed from -6.5 ± 0.4 mV to -8.1 ± 0.5
227 mV ($P < 0.05$; n = 9; paired t test; Figure 5D; Table 2). In summary, both ESL and S-Lic affected
228 various aspects of the voltage dependence characteristics of $Na_v1.5$ in MDA-MB-231 and HEK-
229 $Na_v1.5$ cells, predominantly hyperpolarising the voltage dependence of inactivation.

230 **3.3 Effect of eslicarbazepine acetate and S-licarbazepine on activation and inactivation**
231 **kinetics**

232 We next studied the effect of both compounds on kinetics of activation and inactivation. In MDA-
233 MB-231 cells, ESL significantly accelerated the time to peak current (T_p) upon depolarisation from
234 -120 mV to -10 mV from 2.1 ± 0.2 ms to 1.9 ± 0.2 ms ($P < 0.01$; n = 13; paired t test; Table 1).
235 However, in HEK-$Na_v1.5$ cells, ESL significantly slowed T_p from 1.4 ± 0.2 ms to 1.5 ± 0.2 ms (P <
236 0.001; n = 14; paired t test; Table 1). S-Lic had no significant effect on T_p in MDA-MB-231 cells but
237 significantly slowed T_p in HEK-$Na_v1.5$ cells from 1.8 ± 0.5 ms to 2.3 ± 0.6 ms ($P < 0.01$; n = 13;
238 paired t test; Table 2).

239 To study effects on inactivation kinetics, the current decay following depolarisation from -120 mV to
240 -10 mV was fitted to a double exponential function to derive fast and slow time constants of
241 inactivation (τ_f and τ_s). Neither ESL nor S-Lic had any significant effect on τ_f or τ_s in MDA-MB-231
242 cells (Tables 1, 2). However, in HEK-$Na_v1.5$ cells, ESL significantly slowed τ_f from 0.9 ± 0.1 ms to
243 1.2 ± 0.1 ms ($P < 0.001$; n = 12; paired t test; Table 1) and slowed τ_s from 6.6 ± 0.8 ms to 20.8 ± 8.5
244 ms, although this was not statistically significant. S-Lic significantly slowed τ_f from 1.0 ± 0.04 ms to
245 1.3 ± 0.06 ms ($P < 0.001$; n = 11; paired t test; Table 2) and τ_s from 6.3 ± 0.5 ms to 7.3 ± 0.5 ms (P <
246 0.05; n = 11; paired t test; Table 2). In summary, both ESL and S-Lic elicited various effects on
247 kinetics in MDA-MB-231 and HEK-$Na_v1.5$ cells, predominantly slowing activation and inactivation.

248 **3.4 Use-dependent effect of eslicarbazepine acetate and S-licarbazepine on $Na_v1.5$**

249 To study use-dependent block of Na^+ current by ESL and S-Lic, we ran a protocol where cells were
250 subjected to repeated depolarisations from -120 mV to 0 mV, at a frequency of 50 Hz. In MDA-MB-
251 231 cells, this depolarisation train caused a rapid decrease in current size, which reached a plateau of
252 88.8 ± 2.3 % of the initial current (Figure 6A). In the presence of ESL, the decrease in current
253 reached a plateau of 81.5 ± 2.3 %, suggesting use-dependent block of the channel, although this was
254 not statistically significant (P = 0.10; n = 9; paired t test; Figure 6A). S-Lic had a similar but less
255 obvious effect where the current declined to 80.5 ± 3.1 % in the presence of S-Lic, compared to 86.5
256 ± 3.1 % without drug (P = 0.31; n = 7; paired t test; Figure 6B).

257 Use-dependent block was easier to study in HEK-$Na_v1.5$ cells due to the larger Na^+ current. In these
258 cells, ESL increased the reduction in current amplitude to 60.6 ± 7.9 % of the initial current,
259 compared to 90.0 ± 2.1 % without drug (P < 0.01; n = 9; paired t test; Figure 6C). S-Lic also
260 increased the reduction in current amplitude to 76.1 ± 2.1 % of the initial current, compared to 85.7 ±
261 2.2 % without drug (P < 0.001; n = 9; paired t test; Figure 6D). Together, these results indicate that
262 both ESL and S-Lic cause use-dependent block of $Na_v1.5$ at a stimulation frequency of 50 Hz.

263 **3.5 Effect of eslicarbazepine acetate and S-licarbazepine on recovery from fast inactivation**

264 To investigate the effect of ESL and S-Lic on channel recovery from fast inactivation, we subjected
265 cells to two depolarisations from V_h of -120 mV to 0 mV, changing the interval between these in
266 which the channels were held at -120 mV to facilitate recovery. Significance was determined by
267 fitting a single exponential curve to the normalised current/time relationship and calculating the time
268 constant (τ_r). In MDA-MB-231 cells, ESL significantly slowed τ_r from 6.0 ± 0.5 ms to 8.7 ± 0.7 ms
269 (P < 0.05; n = 10; paired t test; Figure 7A, Table 1). Similarly, in HEK-$Na_v1.5$ cells, ESL
270 significantly slowed τ_r from 4.5 ± 0.4 ms to 7.1 ± 0.6 ms (P < 0.001; n = 10; paired t test; Figure 7B,
271 Table 1). S-Lic also significantly slowed τ_r in MDA-MB-231 cells from 6.8 ± 0.4 ms to 13.5 ± 1.0
272 ms (P < 0.01; n = 7; paired t test; Figure 7C, Table 2). Finally, S-Lic also significantly slowed τ_r in
273 HEK-$Na_v1.5$ cells from 5.7 ± 0.7 ms to 8.0 ± 1.2 ms (P < 0.01; n = 10; paired t test; Figure 7D, Table
274 2). In summary, both ESL and S-Lic slowed recovery from fast inactivation of $Na_v1.5$.

275 **4 Discussion**

276 In this study, we have shown that ESL and its active metabolite S-Lic (both at 300 μM) inhibit the
277 transient and persistent components of Na^+ current carried by $Na_v1.5$. We show broadly similar
278 effects in MDA-MB-231 cells, which express endogenous $Na_v1.5$ (29, 30, 45), and in HEK-293 cells
279 over-expressing $Na_v1.5$. Notably, both compounds were more effective when V_h was set to -80 mV
280 than at -120 mV, suggestive of depolarised state-dependent binding. In addition, the inhibitory effect
281 of ESL was reversible whereas inhibition by S-Lic was not. As regards voltage-dependence, both
282 ESL and S-Lic shifted activation and steady-state inactivation curves, to varying extents in the two
283 cell lines, in the direction of more negative voltages. ESL and S-Lic had various effects on activation
284 and inactivation kinetics, generally slowing the rate of inactivation. Both ESL and S-Lic also caused
285 use-dependent block of $Na_v1.5$, although the effect was more obvious in HEK-$Na_v1.5$ cells due to the
286 larger Na^+ current. Finally, recovery from fast inactivation of $Na_v1.5$ was significantly slowed by
287 both ESL and S-Lic.

288 To our knowledge, this is the first time that the effects of ESL and S-Lic have specifically been tested
289 on the $Na_v1.5$ isoform. A strength of this study is that both the prodrug (ESL) and the active
290 metabolite (S-Lic) were tested using two independent cell lines, one endogenously expressing

291 $Na_v1.5$, the other stably over-expressing $Na_v1.5$. MDA-MB-231 cells also express $Na_v1.7$, although
292 this isoform is estimated to be responsible for only ~9 % of the total VGSC current (30, 45). MDA-
293 MB-231 cells also express endogenous β1, β2 and β4 subunits (47-49). MDA-MB-231 cells
294 predominantly express the developmentally regulated 'neonatal' $Na_v1.5$ splice variant, which differs
295 from the 'adult' variant over-expressed in the HEK-$Na_v1.5$ cells by seven amino acids located in the
296 extracellular linker between transmembrane segments 3 and 4 of domain 1 (30, 42, 45). Notably,
297 however, there were no consistent differences in effect of either ESL or S-Lic between the MDA-
298 MB-231 and HEK-$Na_v1.5$ cells, suggesting that the neonatal vs. adult splicing event, and/or
299 expression of endogenous β subunits, does not impact on sensitivity of $Na_v1.5$ to these compounds.
300 This finding contrasts another report showing different sensitivity of the neonatal and adult $Na_v1.5$
301 splice variants to the amide local anaesthetics lidocaine and levobupivacaine (44). Our findings
302 suggest that the inhibitory effect of S-Lic on $Na_v1.5$ is less reversible than that of ESL. This may be
303 explained by the differing chemical structures of the two molecules possibly enabling S-Lic to bind
304 the target with higher affinity than ESL. Most VGSC-targeting anticonvulsants, including phenytoin,
305 lamotrigine and carbamazepine, block the pore by binding via aromatic-aromatic interaction to a
306 tyrosine and phenylalanine located in the S6 helix of domain 4 (50). However, S-Lic has been
307 proposed to bind to a different site given that it was found to block the pore predominantly during
308 slow inactivation (10). Alternatively, the hydroxyl group present on S-Lic (but not ESL) may become
309 deprotonated, potentially trapping it in the cytoplasm.

310 This study used a single concentration for both compounds (300 μM) and the findings presented here
311 broadly agree with *in vitro* concentrations used elsewhere to study effects of ESL and S-Lic on Na^+
312 currents. For example, using a V_h of -80 mV, 300 μM ESL was shown to inhibit peak Na^+ current by
313 50 % in N1E-115 neuroblastoma cells expressing $Na_v1.1$, $Na_v1.2$, $Na_v1.3$, $Na_v1.6$ and $Na_v1.7$ (20). S-
314 Lic (250 μM) also blocks peak Na^+ current by ~50 % in the same cell line (10). In addition, S-Lic
315 (300 μM) reduces persistent Na^+ current by ~25 % in acutely isolated murine hippocampal CA1
316 neurons expressing $Na_v1.1$, $Na_v1.2$ and $Na_v1.6$ (21-24). Similar to the present study, ESL was shown
317 to hyperpolarise the voltage-dependence of steady-state inactivation in N1E-115 cells (20). On the
318 other hand, similar to our finding in HEK-$Na_v1.5$ cells, S-Lic has no effect on steady-state
319 inactivation in N1E-115 cells (10). Again, in agreement with our own findings for $Na_v1.5$, S-Lic
320 slows recovery from inactivation and causes use-dependent inhibition in N1E-115 cells (10). It
321 should be noted that the frequency of stimulation used in the protocol to assess use-dependent block
322 (50 Hz) is much faster than the typical human heart rate (1-2 Hz), thus, $Na_v1.5$ in cardiac tissue
323 would not be expected to experience use-dependent block to this extent. Nonetheless, these
324 observations suggest that the sensitivity of $Na_v1.5$ to ESL and S-Lic is broadly similar to that
325 reported for neuronal VGSCs. In support of this, $Na_v1.5$ shares the same conserved residues proposed
326 for $Na_v1.2$ to interact with ESL (Figure 8) (51).

327 Notably, the concentration used in this study is high compared with concentrations achieved in
328 clinical use (e.g. ESL 1200 mg QD gives a peak plasma concentration of ~90 μM) (10). However, it
329 has been argued that the relatively high concentrations required for channel inhibition *in vitro* are
330 clinically relevant given that S-Lic has a high (50:1) lipid:water partition co-efficient and thus would
331 be expected to reside predominantly in the tissue membrane fraction *in vivo* (15). Future work
332 investigating the dose-dependent effects of ESL and S-Lic would be useful to resolve these
333 possibilities and aid clinical judgements.

334 The data presented here raise several implications for clinicians. The observed tonic and use-
335 dependent inhibition of $Na_v1.5$ is worthy of note when considering cardiac function in patients
336 receiving ESL (13). Although the QT interval remains unchanged for individuals on ESL treatment,

prolongation of the PR interval has been observed (27). Further work is required to establish whether the basis for this PR prolongation is indeed via $Na_v1.5$ inhibition. In addition, it would be of interest to investigate the efficacy of ESL and S-Lic in the context of heritable arrhythmogenic mutations in *SCN5A*, as well as the possible involvement of the β subunits (24, 26, 52, 53). The findings presented here are also relevant in the context of $Na_v1.5$ expression in carcinoma cells (54). Given that cancer cells have a relatively depolarised V_m, it is likely that $Na_v1.5$ is mainly in the inactivated state with the persistent Na^+ current being functionally predominant (55, 56). Increasing evidence suggests that persistent Na^+ current carried by $Na_v1.5$ in cancer cells contributes to invasion and several studies have shown that other VGSC inhibitors reduce metastasis in preclinical models (29-35, 57). Thus, use-dependent inhibition by ESL would ensure that channels in malignant cells are particularly targeted, raising the possibility that it could be used as an anti-metastatic agent (43). This study therefore paves the way for future investigations into ESL and S-Lic as potential invasion inhibitors.

5 Author Contributions

TL, SC and WB contributed to the conception and design of the work. TL, LB and WB contributed to acquisition, analysis, and interpretation of data for the work. TL, SC and WB contributed to drafting the work and revising it critically for important intellectual content. All authors approved the final version of the manuscript.

6 Abbreviations

ESL, eslicarbazepine acetate; HEK-$Na_v1.5$, HEK-293 cells stably expressing $Na_v1.5$; I-V, current-voltage; k, slope factor; PSS, physiological saline solution; S-Lic, S-licarbazepine, T_p: time to peak current; τ_f: fast time constant of inactivation; τ_s: slow time constant of inactivation; τ_r: time constant of recovery from inactivation; VGSC, voltage-gated Na^+ channel; V_m, membrane potential; V_h, holding potential; V_{peak}: voltage at which current was maximal;V_{rev}, reversal potential; V_{thres}: threshold voltage for activation; $V_{1/2}$, half-activation voltage.

7 Acknowledgements

This work was supported by Cancer Research UK (A25922) and Breast Cancer Now (2015NovPhD572).

8 Conflict of interest statement

The authors declare that the research was conducted in the absence of any commercial or financial relationships that could be construed as a potential conflict of interest.

9 Data availability statement

The datasets used and/or analysed during the current study are available from the corresponding author on reasonable request.

10 References

1. Almeida L, Soares-da-Silva P. Eslicarbazepine acetate (BIA 2-093). Neurotherapeutics. 2007;4(1):88-96.

2. Sperling MR, Abou-Khalil B, Harvey J, Rogin JB, Biraben A, Galimberti CA, et al. Eslicarbazepine acetate as adjunctive therapy in patients with uncontrolled partial-onset seizures:

375 Results of a phase III, double-blind, randomized, placebo-controlled trial. Epilepsia. 2015;56(2):244-
376 53.

377 3. Almeida L, Falcao A, Maia J, Mazur D, Gellert M, Soares-da-Silva P. Single-dose and
378 steady-state pharmacokinetics of eslicarbazepine acetate (BIA 2-093) in healthy elderly and young
379 subjects. J Clin Pharmacol. 2005;45(9):1062-6.

380 4. Almeida L, Minciu I, Nunes T, Butoianu N, Falcão A, Magureanu S-A, et al.
381 Pharmacokinetics, Efficacy, and Tolerability of Eslicarbazepine Acetate in Children and Adolescents
382 With Epilepsy. The Journal of Clinical Pharmacology. 2008;48(8):966-77.

383 5. Perucca E, Elger C, Halász P, Falcão A, Almeida L, Soares-da-Silva P. Pharmacokinetics of
384 eslicarbazepine acetate at steady-state in adults with partial-onset seizures. Epilepsy Res.
385 2011;96(1):132-9.

386 6. Potschka H, Soerensen J, Pekcec A, Loureiro A, Soares-da-Silva P. Effect of eslicarbazepine
387 acetate in the corneal kindling progression and the amygdala kindling model of temporal lobe
388 epilepsy. Epilepsy Res. 2014;108(2):212-22.

389 7. Sierra-Paredes G, Loureiro AI, Wright LC, Sierra-Marcuño G, Soares-da-Silva P. Effects of
390 eslicarbazepine acetate on acute and chronic latrunculin A-induced seizures and extracellular amino
391 acid levels in the mouse hippocampus. BMC Neurosci. 2014;15(1):134.

392 8. Alves G, Figueiredo I, Falcao A, Castel-Branco M, Caramona M, Soares-Da-Silva P.
393 Stereoselective disposition of S- and R-licarbazepine in mice. Chirality. 2008;20(6):796-804.

394 9. Brady K, Hebeisen S, Konrad D, Soares-da-Silva P. The effects of eslicarbazepine, R-
395 licarbazepine, oxcarbazepine and carbamazepine on ion transmission Cav3.2 channels. Epilepsia.
396 2011;52:260.

397 10. Hebeisen S, Pires N, Loureiro AI, Bonifacio MJ, Palma N, Whyment A, et al. Eslicarbazepine
398 and the enhancement of slow inactivation of voltage-gated sodium channels: a comparison with
399 carbamazepine, oxcarbazepine and lacosamide. Neuropharmacology. 2015;89:122-35.

400 11. Brown ME, El-Mallakh RS. Role of eslicarbazepine in the treatment of epilepsy in adult
401 patients with partial-onset seizures. Ther Clin Risk Manag. 2010;6:103-9.

402 12. Galiana GL, Gauthier AC, Mattson RH. Eslicarbazepine Acetate: A New Improvement on a
403 Classic Drug Family for the Treatment of Partial-Onset Seizures. Drugs R D. 2017;17(3):329-39.

404 13. Zaccara G, Giovannelli F, Cincotta M, Carelli A, Verrotti A. Clinical utility of
405 eslicarbazepine: current evidence. Drug Des Devel Ther. 2015;9:781-9.

406 14. Falcao A, Fuseau E, Nunes T, Almeida L, Soares-da-Silva P. Pharmacokinetics, drug
407 interactions and exposure-response relationship of eslicarbazepine acetate in adult patients with
408 partial-onset seizures: population pharmacokinetic and pharmacokinetic/pharmacodynamic analyses.
409 CNS Drugs. 2012;26(1):79-91.

410 15. Bialer M, Soares-da-Silva P. Pharmacokinetics and drug interactions of eslicarbazepine
411 acetate. Epilepsia. 2012;53(6):935-46.

412 16. Catterall WA. Structure and function of voltage-gated sodium channels at atomic resolution.
413 Exp Physiol. 2014;99(1):35-51.

414 17. Goldin AL, Barchi RL, Caldwell JH, Hofmann F, Howe JR, Hunter JC, et al. Nomenclature
415 of voltage-gated sodium channels. Neuron. 2000;28:365-8.

416 18. Brackenbury WJ, Isom LL. Na Channel beta Subunits: Overachievers of the Ion Channel
417 Family. Front Pharmacol. 2011;2:53.

418 19. Van Wart A, Matthews G. Impaired firing and cell-specific compensation in neurons lacking
419 nav1.6 sodium channels. J Neurosci. 2006;26(27):7172-80.

420 20. Bonifacio MJ, Sheridan RD, Parada A, Cunha RA, Patmore L, Soares-da-Silva P. Interaction
421 of the novel anticonvulsant, BIA 2-093, with voltage-gated sodium channels: comparison with
422 carbamazepine. Epilepsia. 2001;42(5):600-8.

423 21. Royeck M, Horstmann MT, Remy S, Reitze M, Yaari Y, Beck H. Role of axonal NaV1.6
424 sodium channels in action potential initiation of CA1 pyramidal neurons. J Neurophysiol.
425 2008;100(4):2361-80.

426 22. Yu FH, Mantegazza M, Westenbroek RE, Robbins CA, Kalume F, Burton KA, et al. Reduced
427 sodium current in GABAergic interneurons in a mouse model of severe myoclonic epilepsy in
428 infancy. Nat Neurosci. 2006;9(9):1142-9.

429 23. Westenbroek RE, Merrick DK, Catterall WA. Differential subcellular localization of the RI
430 and RII Na+ channel subtypes in central neurons. Neuron. 1989;3(6):695-704.

431 24. Doeser A, Soares-da-Silva P, Beck H, Uebachs M. The effects of eslicarbazepine on
432 persistent Na(+) current and the role of the Na(+) channel beta subunits. Epilepsy Res.
433 2014;108(2):202-11.

434 25. Saint DA. The cardiac persistent sodium current: an appealing therapeutic target? Br J
435 Pharmacol. 2008;153(6):1133-42.

436 26. Uebachs M, Opitz T, Royeck M, Dickhof G, Horstmann MT, Isom LL, et al. Efficacy loss of
437 the anticonvulsant carbamazepine in mice lacking sodium channel beta subunits via paradoxical
438 effects on persistent sodium currents. J Neurosci. 2010;30(25):8489-501.

439 27. Vaz-Da-Silva M, Nunes T, Almeida L, Gutierrez MJ, Litwin JS, Soares-Da-Silva P.
440 Evaluation of Eslicarbazepine acetate on cardiac repolarization in a thorough QT/QTc study. J Clin
441 Pharmacol. 2012;52(2):222-33.

442 28. George AL, Jr. Inherited disorders of voltage-gated sodium channels. J Clin Invest.
443 2005;115(8):1990-9.

444 29. Roger S, Besson P, Le Guennec JY. Involvement of a novel fast inward sodium current in the
445 invasion capacity of a breast cancer cell line. Biochim Biophys Acta. 2003;1616(2):107-11.

446 30. Fraser SP, Diss JK, Chioni AM, Mycielska ME, Pan H, Yamaci RF, et al. Voltage-gated
447 sodium channel expression and potentiation of human breast cancer metastasis. Clin Cancer Res.
448 2005;11(15):5381-9.

449 31. House CD, Vaske CJ, Schwartz AM, Obias V, Frank B, Luu T, et al. Voltage-gated Na+
450 channel SCN5A is a key regulator of a gene transcriptional network that controls colon cancer
451 invasion. Cancer Res. 2010;70(17):6957-67.

452 32. Nelson M, Yang M, Millican-Slater R, Brackenbury WJ. Nav1.5 regulates breast tumor
453 growth and metastatic dissemination in vivo. Oncotarget. 2015;6(32):32914-29.

454 33. Nelson M, Yang M, Dowle AA, Thomas JR, Brackenbury WJ. The sodium channel-blocking
455 antiepileptic drug phenytoin inhibits breast tumour growth and metastasis. Mol Cancer.
456 2015;14(1):13.

457 34. Driffort V, Gillet L, Bon E, Marionneau-Lambot S, Oullier T, Joulin V, et al. Ranolazine
458 inhibits NaV1.5-mediated breast cancer cell invasiveness and lung colonization. Mol Cancer.
459 2014;13(1):264.

460 35. Yang M, Kozminski DJ, Wold LA, Modak R, Calhoun JD, Isom LL, et al. Therapeutic
461 potential for phenytoin: targeting Na(v)1.5 sodium channels to reduce migration and invasion in
462 metastatic breast cancer. Breast Cancer Res Treat. 2012;134(2):603-15.

463 36. Simon A, Yang M, Marrison JL, James AD, Hunt MJ, O'Toole PJ, et al. Metastatic breast
464 cancer cells induce altered microglial morphology and electrical excitability in vivo. J
465 Neuroinflammation. 2020;17(1):87.

466 37. Masters JR, Thomson JA, Daly-Burns B, Reid YA, Dirks WG, Packer P, et al. Short tandem
467 repeat profiling provides an international reference standard for human cell lines. Proc Natl Acad Sci
468 U S A. 2001;98(14):8012-7.

469 38. Uphoff CC, Gignac SM, Drexler HG. Mycoplasma contamination in human leukemia cell
470 lines. I. Comparison of various detection methods. J Immunol Methods. 1992;149(1):43-53.

471 39. Brackenbury WJ, Djamgoz MB. Activity-dependent regulation of voltage-gated Na^+ channel
472 expression in Mat-LyLu rat prostate cancer cell line. J Physiol. 2006;573(Pt 2):343-56.

473 40. Armstrong CM, Bezanilla F. Inactivation of the sodium channel. II. Gating current
474 experiments. J Gen Physiol. 1977;70(5):567-90.

475 41. Soares-da-Silva P, Pires N, Bonifácio MJ, Loureiro AI, Palma N, Wright LC. Eslicarbazepine
476 acetate for the treatment of focal epilepsy: an update on its proposed mechanisms of action.
477 Pharmacol Res Perspect. 2015;3(2).

478 42. Djamgoz MBA, Fraser SP, Brackenbury WJ. In Vivo Evidence for Voltage-Gated Sodium
479 Channel Expression in Carcinomas and Potentiation of Metastasis. Cancers (Basel). 2019;11(11).

480 43. Martin F, Ufodiama C, Watt I, Bland M, Brackenbury WJ. Therapeutic value of voltage-gated
481 sodium channel inhibitors in breast, colorectal and prostate cancer: a systematic review. Front
482 Pharmacol. 2015;6:273.

483 44. Elajnaf T, Baptista-Hon DT, Hales TG. Potent Inactivation-Dependent Inhibition of Adult
484 and Neonatal NaV1.5 Channels by Lidocaine and Levobupivacaine. Anesth Analg. 2018;127(3):650-
485 60.

486 45. Brackenbury WJ, Chioni AM, Diss JK, Djamgoz MB. The neonatal splice variant of Nav1.5
487 potentiates in vitro metastatic behaviour of MDA-MB-231 human breast cancer cells. Breast Cancer
488 Res Treat. 2007;101(2):149-60.

489 46. Patino GA, Brackenbury WJ, Bao YY, Lopez-Santiago LF, O'Malley HA, Chen CL, et al.
490 Voltage-Gated Na+ Channel beta 1B: A Secreted Cell Adhesion Molecule Involved in Human
491 Epilepsy. J Neurosci. 2011;31(41):14577-91.

492 47. Nelson M, Millican-Slater R, Forrest LC, Brackenbury WJ. The sodium channel beta1
493 subunit mediates outgrowth of neurite-like processes on breast cancer cells and promotes tumour
494 growth and metastasis. Int J Cancer. 2014;135(10):2338-51.

495 48. Chioni AM, Brackenbury WJ, Calhoun JD, Isom LL, Djamgoz MB. A novel adhesion
496 molecule in human breast cancer cells: voltage-gated Na+ channel beta1 subunit. Int J Biochem Cell
497 Biol. 2009;41(5):1216-27.

498 49. Bon E, Driffort V, Gradek F, Martinez-Caceres C, Anchelin M, Pelegrin P, et al. SCN4B acts
499 as a metastasis-suppressor gene preventing hyperactivation of cell migration in breast cancer. Nature
500 communications. 2016;7:13648.

501 50. Lipkind GM, Fozzard HA. Molecular model of anticonvulsant drug binding to the voltage-
502 gated sodium channel inner pore. Mol Pharmacol. 2010;78(4):631-8.

503 51. Shaikh S, Rizvi SM, Hameed N, Biswas D, Khan M, Shakil S, et al. Aptiom (eslicarbazepine
504 acetate) as a dual inhibitor of beta-secretase and voltage-gated sodium channel: advancement in
505 Alzheimer's disease-epilepsy linkage via an enzoinformatics study. CNS Neurol Disord Drug
506 Targets. 2014;13(7):1258-62.

507 52. Brackenbury WJ, Isom LL. Voltage-gated Na+ channels: potential for beta subunits as
508 therapeutic targets. Expert Opin Ther Targets. 2008;12(9):1191-203.

509 53. Rivaud MR, Delmar M, Remme CA. Heritable arrhythmia syndromes associated with
510 abnormal cardiac sodium channel function: ionic and non-ionic mechanisms. Cardiovasc Res. 2020.

511 54. Fraser SP, Ozerlat-Gunduz I, Brackenbury WJ, Fitzgerald EM, Campbell TM, Coombes RC,
512 et al. Regulation of voltage-gated sodium channel expression in cancer: hormones, growth factors
513 and auto-regulation. Philos Trans R Soc Lond B Biol Sci. 2014;369(1638):20130105.

514 55. Yang M, Brackenbury WJ. Membrane potential and cancer progression. Front Physiol.
515 2013;4:185.

516 56. Yang M, James AD, Suman R, Kasprowicz R, Nelson M, O'Toole PJ, et al. Voltage-
517 dependent activation of Rac1 by Nav 1.5 channels promotes cell migration. J Cell Physiol.
518 2020;235(4):3950-72.

519 57. Besson P, Driffort V, Bon E, Gradek F, Chevalier S, Roger S. How do voltage-gated sodium
520 channels enhance migration and invasiveness in cancer cells? Biochim Biophys Acta. 2015;1848(10
521 Pt B):2493-501.

522

523 **10.1 Figure legends**

524 **Figure 1.** Chemical structures of eslicarbazepine acetate and S-licarbazepine. (A) eslicarbazepine
525 acetate; (9S)-2-carbamoyl-2-azatricyclo[9.4.0.0^{3,8}]pentadeca-1(15),3,5,7,11,13-hexaen-9-yl acetate.
526 (B) S-licarbazepine; (10R)-10-hydroxy-2-azatricyclo[9.4.0.0^{3,8}]pentadeca-1(11),3,5,7,12,14-hexaene-
527 2-carboxamide. Structures were drawn using Chemspider software.

528 **Figure 2.** Effect of eslicarbazepine acetate on $Na_v1.5$ currents. (A) Representative Na^+ currents in an
529 MDA-MB-231 cell elicited by a depolarisation from -120 mV to -10 mV in physiological saline
530 solution (PSS; black), eslicarbazepine acetate (ESL; 300 µM; red) and after washout (grey). Dotted
531 vertical lines define the persistent Na^+ currents shown in (B). (B) Representative persistent Na^+
532 currents in an MDA-MB-231 cell elicited by a depolarisation from -120 mV to -10 mV. (C)
533 Representative Na^+ currents in an MDA-MB-231 cell elicited by a depolarisation from -80 mV to -10
534 mV. (D) Normalised Na^+ currents in MDA-MB-231 cells elicited by a depolarisation from -120 mV
535 to -10 mV. (E) Normalised Na^+ currents in MDA-MB-231 cells elicited by a depolarisation from -80
536 mV to -10 mV. (F) Representative Na^+ currents in a HEK-$Na_v1.5$ cell elicited by a depolarisation
537 from -120 mV to -10 mV in PSS (black), ESL (300 µM; red) and after washout (grey). Dotted
538 vertical lines define the persistent Na^+ currents shown in (G). (G) Representative persistent Na^+
539 currents in a HEK-$Na_v1.5$ cell elicited by a depolarisation from -120 mV to -10 mV. (H)

540 Representative Na^+ currents in a HEK-$Na_v1.5$ cell elicited by a depolarisation from -80 mV to -10
541 mV. (I) Normalised Na^+ currents in HEK-$Na_v1.5$ cells elicited by a depolarisation from -120 mV to -
542 10 mV. (J) Normalised Na^+ currents in HEK-$Na_v1.5$ cells elicited by a depolarisation from -80 mV to
543 -10 mV. Results are mean + SEM. **P ≤ 0.01; ***P ≤ 0.001; one-way ANOVA with Tukey tests (n
544 = 12-14). NS, not significant.

545 **Figure 3.** Effect of S-licarbazepine on $Na_v1.5$ currents. (A) Representative Na^+ currents in an MDA-
546 MB-231 cell elicited by a depolarisation from -120 mV to -10 mV in physiological saline solution
547 (PSS; black), S-licarbazepine (S-Lic; 300 μM; red) and after washout (grey). Dotted vertical lines
548 define the persistent Na^+ currents shown in (B). (B) Representative persistent Na^+ currents in an
549 MDA-MB-231 cell elicited by a depolarisation from -120 mV to -10 mV. (C) Representative Na^+
550 currents in an MDA-MB-231 cell elicited by a depolarisation from -80 mV to -10 mV. (D)
551 Normalised Na^+ currents in MDA-MB-231 cells elicited by a depolarisation from -120 mV to -10
552 mV. (E) Normalised Na^+ currents in MDA-MB-231 cells elicited by a depolarisation from -80 mV to
553 -10 mV. (F) Representative Na^+ currents in a HEK-$Na_v1.5$ cell elicited by a depolarisation from -120
554 mV to -10 mV in PSS (black), S-Lic (300 μM; red) and after washout (grey). Dotted vertical lines
555 define the persistent Na^+ currents shown in (G). (G) Representative persistent Na^+ currents in a HEK-
556 $Na_v1.5$ cell elicited by a depolarisation from -120 mV to -10 mV. (H) Representative Na^+ currents in
557 a HEK-$Na_v1.5$ cell elicited by a depolarisation from -80 mV to -10 mV. (I) Normalised Na^+ currents
558 in HEK-$Na_v1.5$ cells elicited by a depolarisation from -120 mV to -10 mV. (J) Normalised Na^+
559 currents in HEK-$Na_v1.5$ cells elicited by a depolarisation from -80 mV to -10 mV. Results are mean
560 + SEM. *P ≤ 0.05; ***P ≤ 0.001; one-way ANOVA with Tukey tests (n = 9-13). NS, not significant.

561 **Figure 4.** Effect of eslicarbazepine acetate and S-licarbazepine on the current-voltage relationship.
562 (A) Current-voltage (I-V) plots of Na^+ currents in MDA-MB-231 cells in physiological saline
563 solution (PSS; black circles) and in eslicarbazepine acetate (ESL; 300 μM; red squares). (B) (I-V)
564 plots of Na^+ currents in HEK-$Na_v1.5$ cells in PSS (black circles) and ESL (300 μM; red squares). (C)
565 I-V plots of Na^+ currents in MDA-MB-231 cells in PSS (black circles) and S-licarbazepine (S-Lic;
566 300 μM; red squares). (D) I-V plots of Na^+ currents in HEK-$Na_v1.5$ cells in PSS (black circles) and
567 S-Lic (300 μM; red squares). Currents were elicited using 10 mV depolarising steps from -80 to +30
568 mV for 30 ms, from a holding potential of -120 mV. Results are mean ± SEM (n = 7-13).

569 **Figure 5.** Effect of eslicarbazepine acetate and S-licarbazepine on activation and steady-state
570 inactivation. (A) Activation and steady-state inactivation in MDA-MB-231 cells in physiological
571 saline solution (PSS; black circles) and in eslicarbazepine acetate (ESL; 300 μM; red squares). (B)
572 Activation and steady-state inactivation in HEK-$Na_v1.5$ cells in PSS (black circles) and ESL (300
573 μM; red squares). (C) Activation and steady-state inactivation in MDA-MB-231 cells in PSS (black
574 circles) and S-licarbazepine (S-Lic; 300 μM; red squares). (D) Activation and steady-state
575 inactivation in HEK-$Na_v1.5$ cells in PSS (black circles) and S-Lic (300 μM; red squares). For
576 activation, normalised conductance (G/G_{max}) was calculated from the current data and plotted as a
577 function of voltage. For steady-state inactivation, normalised current (I/I_{max}), elicited by 50 ms test
578 pulses at -10 mV following 250 ms conditioning voltage pulses between -120 mV and +30 mV,
579 applied from a holding potential of -120 mV, was plotted as a function of the prepulse voltage.
580 Results are mean ± SEM (n = 7-13). Activation and inactivation curves are fitted with Boltzmann
581 functions.

582 **Figure 6.** Use-dependent block by eslicarbazepine acetate and S-licarbazepine. (A) Rundown of Na^+
583 current in MDA-MB-231 cells in physiological saline solution (PSS; black circles) and in
584 eslicarbazepine acetate (ESL; 300 μM; red squares). (B) Rundown of Na^+ current in MDA-MB-231

585 cells in PSS (black circles) and S-licarbazepine (S-Lic; 300 μM; red squares). (C) Rundown of Na^+
586 current in HEK-$Na_v1.5$ cells in PSS (black circles) and ESL (300 μM; red squares). (D) Rundown of
587 Na^+ current in HEK-$Na_v1.5$ cells in PSS (black circles) and S-Lic (300 μM; red squares). Currents
588 were elicited by 50 Hz pulse trains to 0 mV, applied from a holding potential of -120 mV, normalised
589 to the current evoked by the first pulse plotted as a function of the pulse number. Data are fitted with
590 single exponential functions. Results are mean ± SEM (n = 7-10).

591 **Figure 7.** Effect of eslicarbazepine acetate and S-licarbazepine on recovery from inactivation. (A)
592 Recovery from inactivation in MDA-MB-231 cells in physiological saline solution (PSS; black
593 circles) and in eslicarbazepine acetate (ESL; 300 μM; red squares). (B) Recovery from inactivation in
594 HEK-$Na_v1.5$ cells in PSS (black circles) and ESL (300 μM; red squares). (C) Recovery from
595 inactivation in MDA-MB-231 cells in PSS (black circles) and S-licarbazepine (S-Lic; 300 μM; red
596 squares). (D) Recovery from inactivation in HEK-$Na_v1.5$ cells in PSS (black circles) and S-Lic (300
597 μM; red squares). The fraction recovered (I_t/I_c) was determined by a 25 ms pulse to 0 mV (I_c),
598 followed by a recovery pulse to -120 mV for 1-500 ms, and a subsequent 25 ms test pulse to 0 mV
599 (I_t), applied from a holding potential of -120 mV, and plotted as a function of the recovery interval.
600 Data are fitted with single exponential functions which are statistically different between control and
601 drug treatments in all cases. Results are mean ± SEM (n = 7-10).

602 **Figure 8.** Clustal alignment of amino acid sequences of $Na_v1.1$-$Na_v1.9$ (*SCN1A-SCN11A*). ESL was
603 proposed previously (51) to interact with the highlighted amino acids in $Na_v1.2$. An alignment of
604 $Na_v1.2$ (UniProtKB - Q99250 (SCN2A_HUMAN)) with $Na_v1.1$ (UniProtKB - P35498
605 (SCN1A_HUMAN)), $Na_v1.3$ (UniProtKB - Q9NY46 (SCN3A_HUMAN)), $Na_v1.4$ (UniProtKB -
606 P35499 (SCN4A_HUMAN)), $Na_v1.5$ (UniProtKB - Q14524 (SCN5A_HUMAN)) $Na_v1.6$
607 (UniProtKB - Q9UQD0 (SCN8A_HUMAN)), $Na_v1.7$ (UniProtKB - Q15858 (SCN9A_HUMAN)),
608 $Na_v1.8$ (UniProtKB - Q9Y5Y9 (SCN10A_HUMAN)), and $Na_v1.9$ (UniProtKB - Q9UI33
609 (SCN11A_HUMAN)) shows that the interacting amino acids highlighted in yellow are conserved
610 between $Na_v1.2$ and $Na_v1.5$, along with most other isoforms. Asterisks indicate conserved residues.
611 Colon indicates conservation between groups of strongly similar properties - scoring > 0.5 in the
612 Gonnet PAM 250 matrix. Period indicates conservation between groups of weakly similar properties
613 - scoring ≤ 0.5 in the Gonnet PAM 250 matrix.

614

615 **Table 1.** Effect of eslicarbazepine acetate on Na^+ current characteristics in MDA-MB-231 and HEK-
616 $Na_v1.5$ cells.[1]

A. MDA-MB-231 cells				
Parameter	*Control*	*ESL*	*P value*	*N*
V_{thres} (mV)	-45.7 ± 1.7	-45.0 ± 1.4	0.58	13
V_{peak} (mV)	3.1 ± 2.1	-3.9 ± 2.7	0.056	13
Activation V½ (mV)	-19.3 ± 1.4	-22.0 ± 1.5	0.095	12
Activation k (mV)	10.6 ± 0.7	9.3 ± 0.8	0.076	12
Inactivation V½ (mV)	-80.6 ± 0.7	-86.7 ± 1.2	<0.001	13
Inactivation k (mV)	-4.8 ± 0.4	-7.4 ± 1.7	0.139	13
Peak current density at -10 mV (pA/pF)	-14.8 ± 3.9	-8.0 ± 2.5	<0.001	13
Persistent current density at -10 mV (pA/pF)	-0.15 ± 0.05	-0.02 ± 0.07	0.13	12
T_p at -10 mV (ms)	2.1 ± 0.2	1.9 ± 0.2	<0.01	13
τ_f at -10 mV (ms)	1.3 ± 0.1	1.3 ± 0.2	0.954	13
τ_s at -10 mV) (ms)	10.0 ± 2.3	6.9 ± 2.0	0.289	13
τ_r (ms)	6.0 ± 0.5	8.7 ± 0.7	<0.05	10
B. HEK-$Na_v1.5$ cells				
Parameter	*Control*	*ESL*	*P value*	*N*
V_{thres} (mV)	-55.0 ± 1.7	-54.0 ± 2.2	0.758	10
V_{peak} (mV)	-26.0 ± 2.2	-24.0 ± 4.3	0.591	10
Activation V½ (mV)	-39.4 ± 1.3	-44.2 ± 1.8	<0.05	10
Activation k (mV)	5.3 ± 1.3	3.8 ± 0.7	0.361	10
Inactivation V½ (mV)	-78.2 ± 2.5	-88.3 ± 2.7	<0.001	10
Inactivation k (mV)	-6.9 ± 0.4	-9.8 ± 0.7	<0.001	10
Peak current density at -10 mV (pA/pF)	-154.4 ± 24.0	-33.1 ± 4.7	<0.001	12
Persistent current density at -10 mV (pA/pF)	-0.61 ± 0.15	-0.12 ± 0.05	<0.01	12
T_p at -10 mV (ms)	1.4 ± 0.2	1.9 ± 0.2	<0.001	14
τ_f at -10 mV (ms)	0.9 ± 0.1	1.2 ± 0.1	<0.001	12
τ_s at -10 mV (ms)	6.6 ± 0.8	20.8 ± 8.5	0.128	12
τ_r (ms)	4.5 ± 0.4	7.1 ± 0.6	<0.001	10

617 [1]ESL: eslicarbazepine acetate (300 μM); V_{thres}: threshold voltage for activation; V_{peak}: voltage at
618 which current was maximal; V½: half (in)activation voltage; k: slope factor for (in)activation; T_p:
619 time to peak current; τ_f: fast time constant of inactivation; τ_s: slow time constant of inactivation; τ_r:
620 time constant of recovery from inactivation. The holding potential was -120 mV. Results are mean ±
621 SEM. Statistical comparisons were made with paired t-tests.

622 **Table 2.** Effect of S-licarbazepine on Na^+ current characteristics in MDA-MB-231 and HEK-$Na_v1.5$
623 cells.[1]

A. MDA-MB-231 cells				
Parameter	*Control*	*S-Lic*	*P value*	*N*
V_{thres} (mV)	-34.4 ± 2.0	-35.7 ± 2.0	0.603	7
V_{peak} (mV)	11.43 ± 4.4	10.0 ± 4.9	0.818	7
Activation V½ (mV)	-12.9 ± 1.3	-13.7 ± 1.4	0.371	7
Activation k (mV)	11.0 ± 0.5	11.9 ± 0.8	0.520	7
Inactivation V½ (mV)	-71.8 ± 2.5	-76.8 ± 2.2	<0.05	7
Inactivation k (mV)	-6.8 ± 0.9	-6.0 ± 1.2	0.302	7
Peak current density at -10 mV (pA/pF)	-12.0 ± 3.1	-6.9 ± 2.5	<0.001	9
Persistent current density at -10 mV (pA/pF)	-1.3 ± 0.4	-0.6 ± 0.2	<0.05	9
T_p at -10 mV (ms)	4.5 ± 0.4	5.1 ± 0.7	0.103	9
τ_f at -10 mV (ms)	3.8 ± 1.1	3.2 ± 0.4	0.553	7
τ_s at -10 mV (ms)	25.7 ± 7.0	27.1 ± 12.0	0.920	7
τ_r (ms)	6.8 ± 0.4	13.5 ± 1.0	<0.01	7
B. HEK-$Na_v1.5$ cells				
Parameter	*Control*	*S-Lic*	*P value*	*N*
V_{thres} (mV)	-50.0 ± 1.9	-51.3 ± 3.5	0.598	9
V_{peak} (mV)	-18.0 ± 4.2	-30.0 ± 5.6	<0.001	9
Activation V½ (mV)	-32.8 ± 3.1	-40.5 ± 3.4	<0.01	9
Activation k (mV)	5.9 ± 0.9	4.5 ± 1.1	<0.05	9
Inactivation V½ (mV)	-75.9 ± 2.6	-79.3 ± 4.1	0.116	9
Inactivation k (mV)	-6.5 ± 0.4	-8.1 ± 0.5	<0.05	9
Peak current density at -10 mV (pA/pF)	-140.9 ± 26.8	-77.2 ± 17.0	<0.001	13
Persistent current density at -10 mV (pA/pF)	-0.9 ± 0.2	-0.5 ± 0.2	<0.05	11
T_p at -10 mV (ms)	1.8 ± 0.5	2.3 ± 0.6	<0.01	13
τ_f at -10 mV (ms)	1.0 ± 0.04	1.3 ± 0.06	<0.001	11
τ_s at -10 mV (ms)	6.3 ± 0.5	7.3 ± 0.5	<0.05	11
τ_r (ms)	5.7 ± 0.7	8.0 ± 1.2	<0.01	10

624 [1]S-Lic: S-licarbazepine (300 μM); V_{thres}: threshold voltage for activation; V_{peak}: voltage at which
625 current was maximal; V½: half (in)activation voltage; k: slope factor for (in)activation; T_p: time to
626 peak current; τ_f: fast time constant of inactivation; τ_s: slow time constant of inactivation; τ_r: time
627 constant of recovery from inactivation. The holding potential was -120 mV. Results are mean ± SEM.
628 Statistical comparisons were made with paired t-tests.

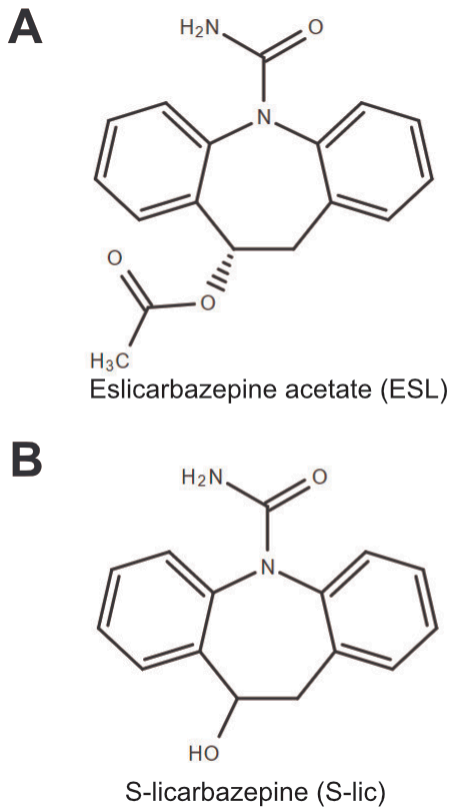

629

630 Figure 1

631

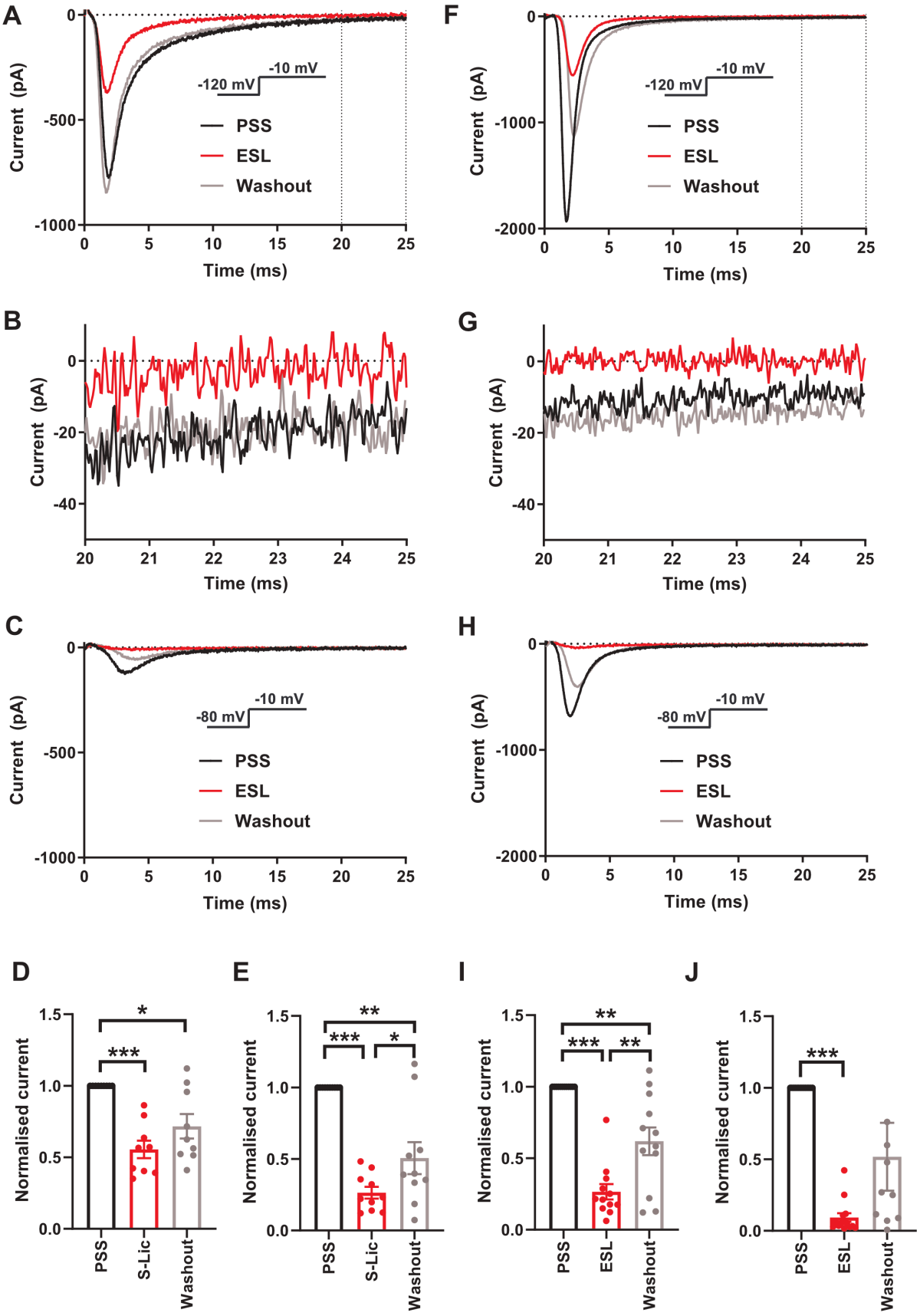

632

633 Figure 2

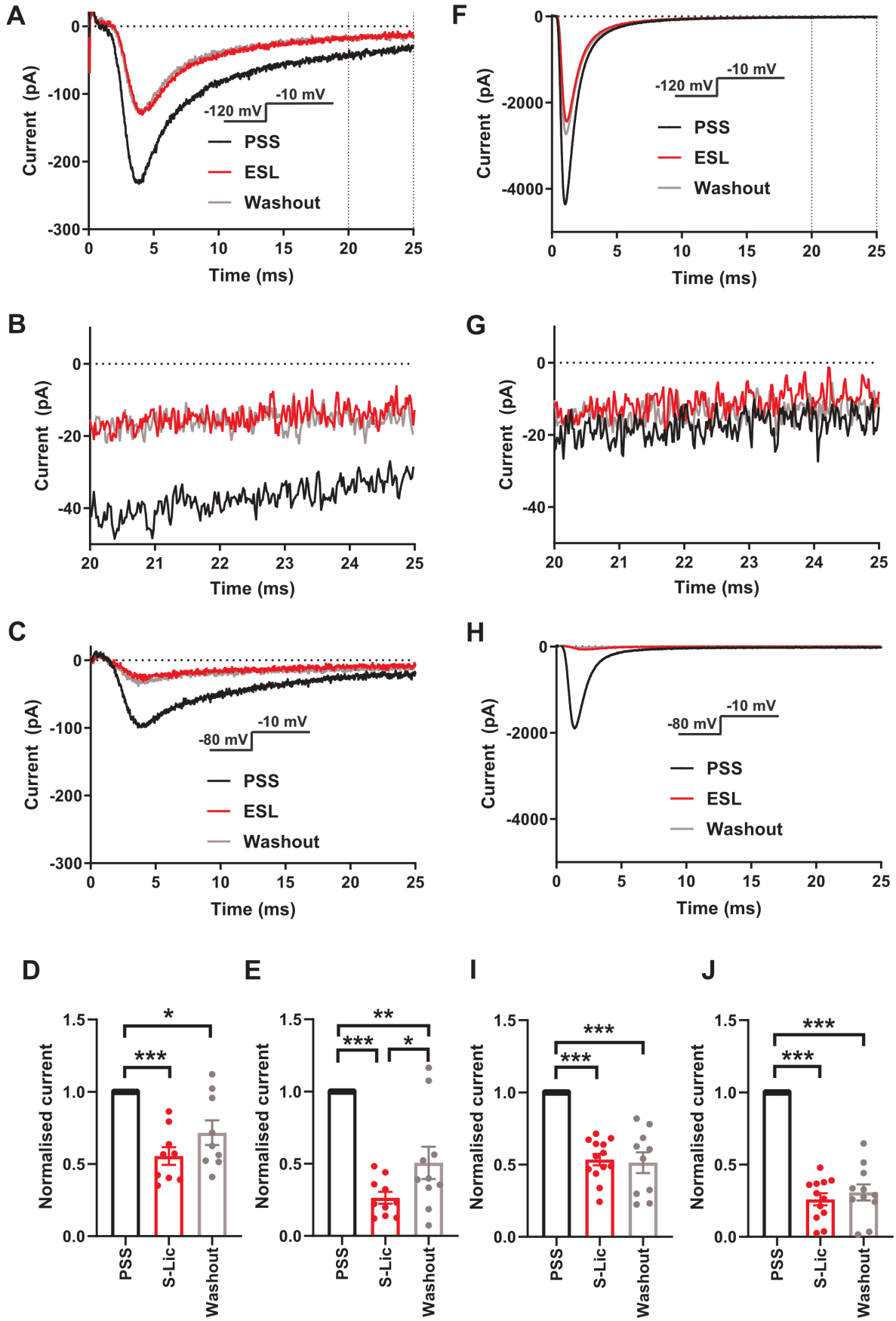

634

635 Figure 3

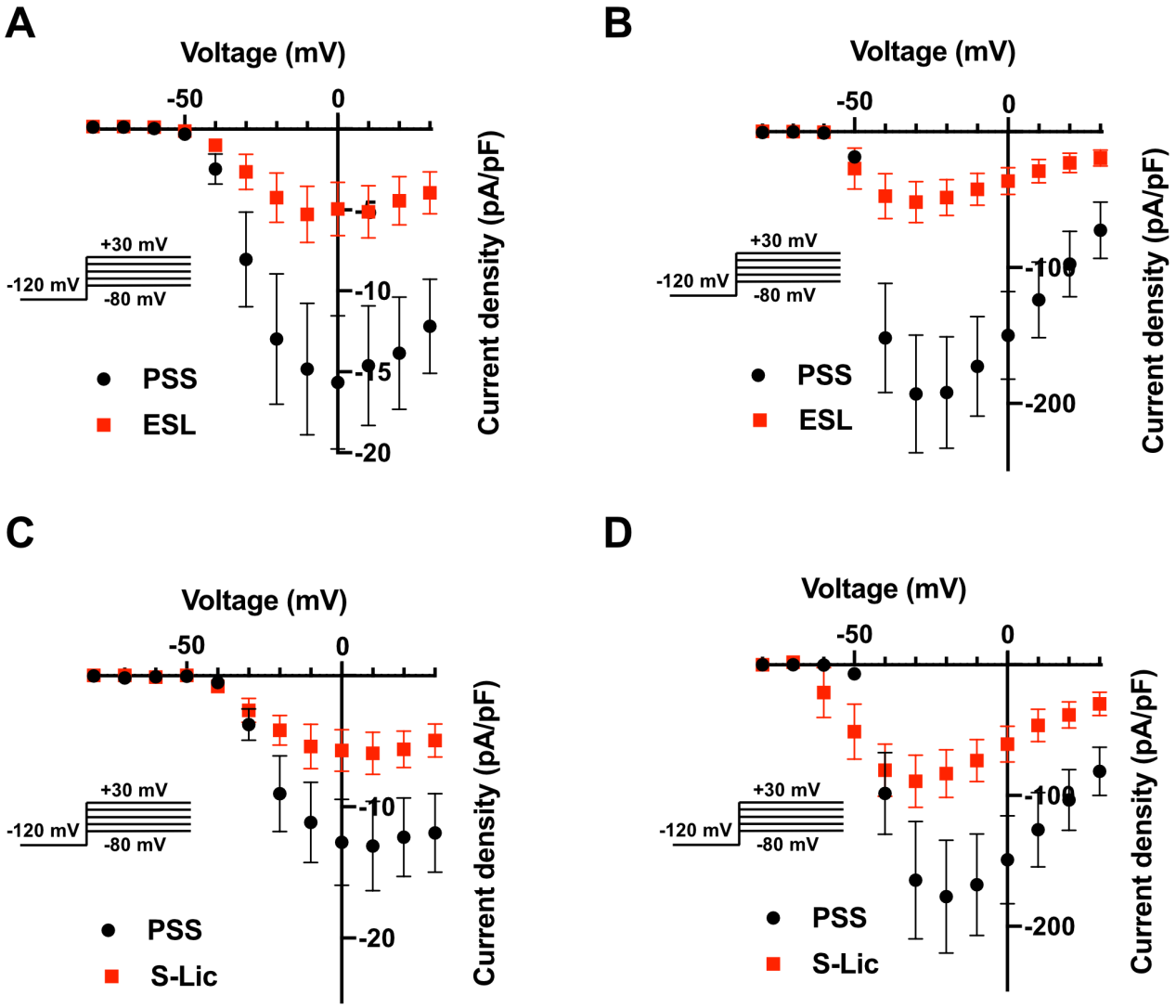
A
Voltage (mV)
-50
0
+30 mV
-120 mV
-80 mV
-10
-15
-20
PSS
ESL
Current density (pA/pF)
B
Voltage (mV)
-50
0
+30 mV
-120 mV
-80 mV
-100
-200
PSS
ESL
Current density (pA/pF)
C
Voltage (mV)
-50
0
+30 mV
-120 mV
-80 mV
-10
-20
PSS
S-Lic
Current density (pA/pF)
D
Voltage (mV)
-50
0
+30 mV
-120 mV
-80 mV
-100
-200
PSS
S-Lic
Current density (pA/pF)

Figure 4

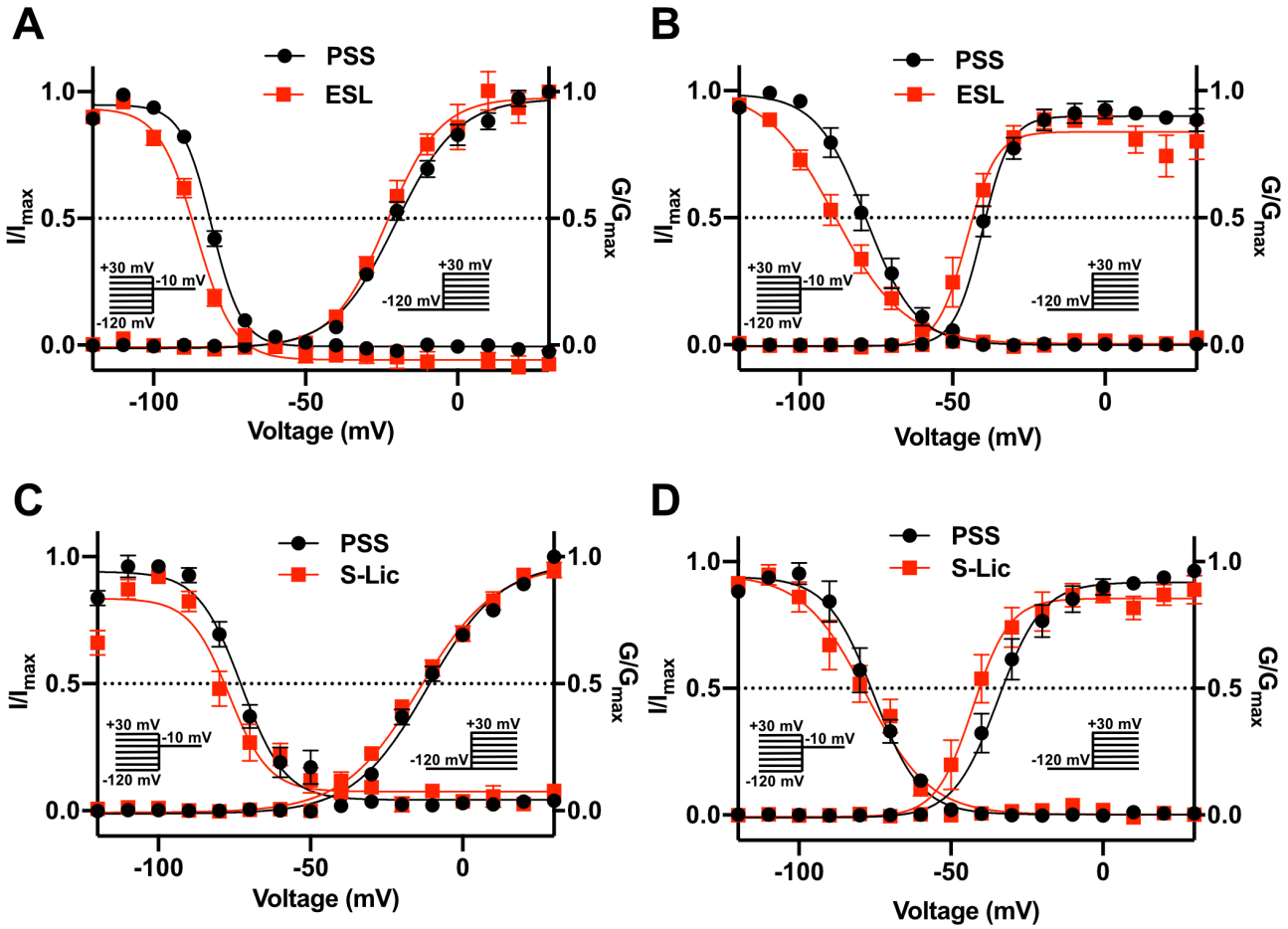

639

640 Figure 5

641

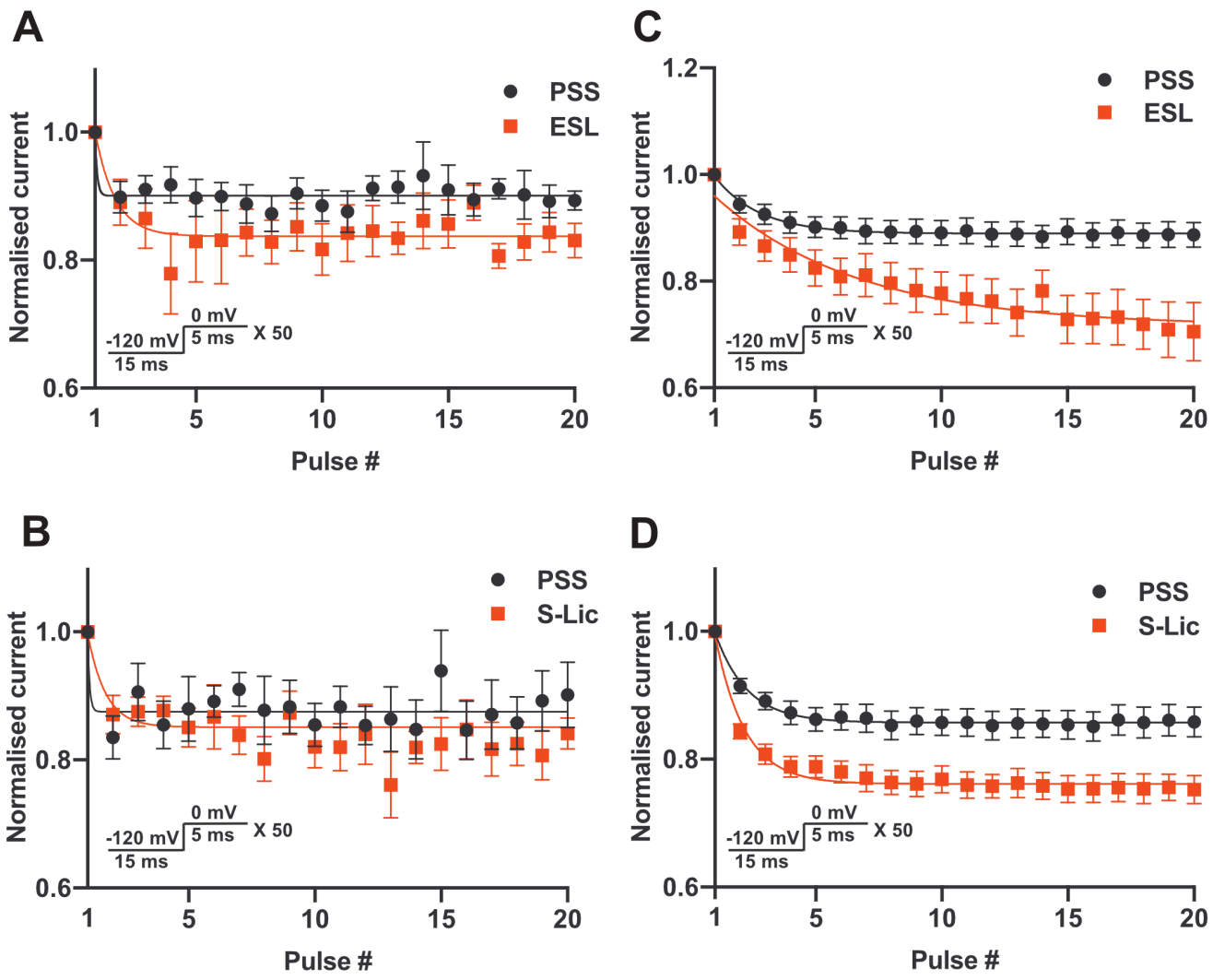

642

643 Figure 6

644

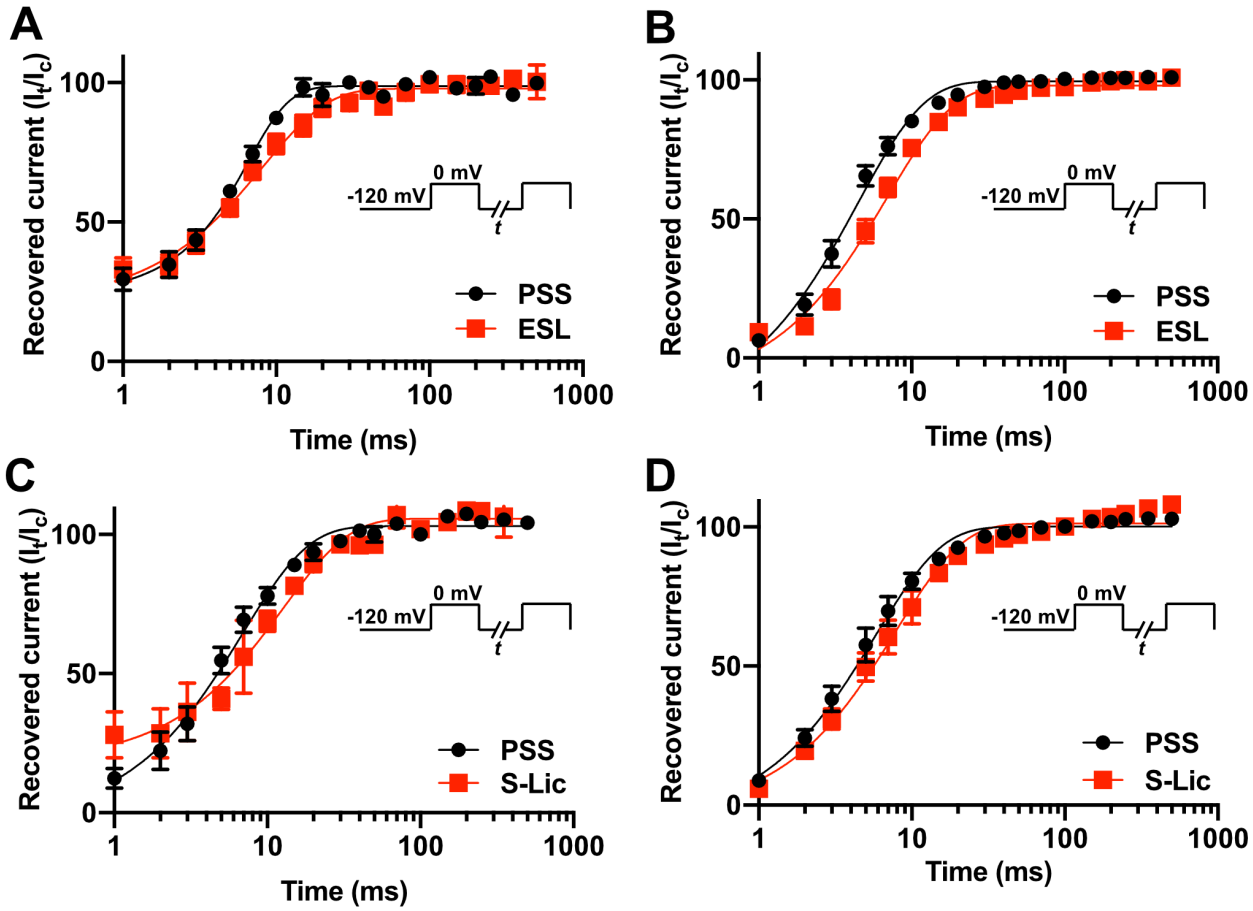

645

646 Figure 7

647

```
SCN1A      ILENFSVATEESAEPLSEDDFEMFYEVWEKFDPDATQFMEFEKLSQFAAALEPPLNLPQP    1844
SCN2A      ILENFSVATEESAEPLSEDDFEMFYEVWEKFDPDATQFIEFAKLSDFADALDPPLLIAKP    1834
SCN3A      ILENFSVATEESAEPLSEDDFEMFYEVWEKFDPDATQFIEFSKLSDFAAALDPPLLIAKP    1829
SCN4A      ILENFNVATEESSEPLGEDDFEMFYETWEKFDPDATQFIAYSRLSDFVDTLQEPLRIAKP    1656
SCN5A      ILENFSVATEESTEPLSEDDFDMFYEIWEKFDPEATQFIEYSVLSDFADALSEPLRIAKP    1830
SCN8A      ILENFSVATEESADPLSEDDFETFYEIWEKFDPDATQFIEYCKLADFADALEHPLRVPKP    1824
SCN9A      ILENFSVATEESTEPLSEDDFEMFYEVWEKFDPDATQFIEFSKLSDFAAALDPPLLIAKP    1818
SCN10A     ILENFNVATEESTEPLSEDDFDMFYETWEKFDPEATQFITFSALSDFADTLSGPLRIPKP    1780
SCN11A     ILENFNTATEESEDPLGEDDFDIFYEVWEKFDPEATQFIKYSALSDFADALPEPLRVAKP    1662
           *****..***** :**.****: *** ******:****: :  *::*. :*  ** : :*

SCN1A      NKLQLIAMDLPMVSGDRIHCLDILFAFTKRVLGESGEMDALRIQMEERFMASNPSKVSYQ    1904
SCN2A      NKVQLIAMDLPMVSGDRIHCLDILFAFTKRVLGESGEMDALRIQMEERFMASNPSKVSYE    1894
SCN3A      NKVQLIAMDLPMVSGDRIHCLDILFAFTKRVLGESGEMDALRIQMEDRFMASNPSKVSYE    1889
SCN4A      NKIKLITLDLPMVPGDKIHCLDILFALTKEVLGDSGEMDALKQTMEEKFMAANPSKVSYE    1716
SCN5A      NQISLINMDLPMVSGDRIHCMDILFAFTKRVLGESGEMDALKIQMEEKFMAANPSKISYE    1890
SCN8A      NTIELIAMDLPMVSGDRIHCLDILFAFTKRVLGDSGELDILRQQMEERFVASNPSKVSYE    1884
SCN9A      NKVQLIAMDLPMVSGDRIHCLDILFAFTKRVLGESGEMDSLRSQMEERFMSANPSKVSYE    1878
SCN10A     NRNILIQMDLPLVPGDKIHCLDILFAFTKNVLGESGELDSLKANMEEKFMATNLSKSSYE    1840
SCN11A     NKYQFLVMDLPMVSEDRLHCMDILFAFTARVLGGSDGLDSMKAMMEEKFMEANPLKKLYE    1722
           *   :: :***:*  *::**:*****:* .*** *. :* ::  **::*: :*  *  *:
```

Figure 8